Study on the Micro-structures of Long Fiber through Runner and Cavity in Injection Molding for Reinforced Thermoplastics (FRT)

Chao-Tsai (CT) Huang[1], Xiang-Lan Peng[2], Sheng-Jye Hwang[2], Huan-Chang Tseng[3], and Rong-Yeu Chang[3]*

1. Chemical and Materials Engineering Department, Energy and Opto-Electronic Materials Research Center, Tamkang University, Taipei, Taiwan

2. Department of Mechanical Engineering, National Cheng Kung University, Tainan, Taiwan

3. R and D Division, CoreTech System (Moldex3D) Co., Ltd., Hsinchu, Taiwan

**Corresponding author: cthuang@mail.tku.edu.tw; cthuang@moldex3d.com*

Abstract

Lightweight technology has been applied into many industries especially for automotive to enhance the fuel efficiency. One of most famous methods is applied fiber-reinforced thermoplastics (FRT) technology, it includes short and long fiber-reinforced thermoplastics (FRT) to support lightweight technology. However, the enhancement mechanism by the microstructures of the fibers in FRT is still too complicated to understand. In this study, we designed a benchmark to study the fiber microstructures based on ASTM D638 with dog-bond system. First, we have tried to study how the geometry of cavity influences the fiber orientation during the injection processes. Furthermore, we have paid the attention on the variation of the fiber length distribution as the injection molding processing. Results show that the geometry of cavity has significant effect on the fiber orientation during the injection processes. Since the system has contraction and expansion structure, the orientation tensor component $\mathbf{a}_{11}$ corresponding to the flow direction, will be enhanced and then decreased along the cavity. Moreover, the fiber lengths have dramatically sharp distribution on skin layer when melt goes through the gate into the cavity. It will allow almost 90% lengths are broken through the skin layer. Meanwhile, using numerical visualization from runner to cavity through core layer, there is about 30% length broken during the journey in runner section. Finally, some fiber orientation results are compared with some literature's. Results showed that our numerical predictions are matched with that of literature quite well in the trend.

Introduction

Lightweight technology has been applied into many industries especially for automotive to enhance the fuel efficiency. One of most famous methods is applied fiber-reinforced thermoplastics technology, it includes short and long fiber-reinforced thermoplastics (FRT) to support lightweight technology. The reason why FRT can be utilized greatly to improve mechanical properties of injection molding products in automotive is due to the functions of fiber microstructure variables, including orientation, length, and concentration. Those microstructure variables will further influence final shrinkage/warpage of with anisotropy. Since the microstructures of fiber inside plastic matrix are very complex, they are not easy to be visualized. Besides, there are too many combination for material, process conditions, the features of microstructures are too complicated to manage and control during the injection molding though the runner, the gate, and then into the cavity. Moreover, some advantages are developing by combining the microcellular and the micro-structures of the long fiber recently [10-11]. It is no doubt that the fiber microstructures prediction and management in FRTs application are still hot in academia and industries [1-4, 8-9].

In this study, we have designed a benchmark to study the fiber microstructures based on ASTM D638 with dog-bond structure. First, we tried to study how the geometry of cavity affects the fiber orientation behavior during the injection processes quantitatively. Furthermore, we have paid more attention on the variation of the fiber length distribution as the injection molding processing. Specifically, we tried to figure out where the long fiber has been damaged significantly. Finally, to verify our simulation results, some literature's results were adopted for confirmation.

Numerical Theory and Background

FRT melt is a concentrated suspension mixture, consisting of fibers and polymer matrix, as assumed to be Generalized Newtonian Fluid (GNF). For the sake of completeness, we give only a brief description of theoretical basis, involving the flow governing equations and the fiber suspension models of fiber orientation, fiber attrition, and fiber migration

I. Injection Molding Simulation Model

The polymer melt is assumed as General Newtonian Fluid (GNF). Hence the non-isothermal 3D flow motion can be mathematically described by the following:

$$\frac{\partial \rho}{\partial t} + \nabla \cdot \rho \mathbf{u} = 0 \qquad (1)$$

$$\frac{\partial}{\partial t}(\rho\mathbf{u}) + \nabla\cdot(\rho\mathbf{u}\mathbf{u} - \boldsymbol{\sigma}) = \rho\mathbf{g} \quad (2)$$

$$\boldsymbol{\sigma} = -p\mathbf{I} + \eta\left(\nabla\mathbf{u} + \nabla\mathbf{u}^T\right) \quad (3)$$

$$\rho C_P\left(\frac{\partial T}{\partial t} + \mathbf{u}\cdot\nabla T\right) = \nabla\cdot(k\nabla T) + \eta\dot{\gamma}^2 \quad (4)$$

where **u** is the velocity vector, T is the temperature, t is the time, p is the pressure, $\boldsymbol{\sigma}$ is the total stress tensor, ρ is the density, η is the viscosity, k is the thermal conductivity, C_p is the specific heat and $\dot{\gamma}$ is the shear rate. The Finite Volume Method (FVM) due to its robustness and efficiency is employed in this study to solve the transient flow field in complex three-dimensional geometry.

II. Fiber orientation model

The fiber orientation is described in detailed by Ref. [2-3]. A *single* fiber is regarded as an axisymmetric bond with rigidness. The bond's unit vector **p** along its axis direction can described as the fiber orientation. Orientation state of a *group* of fibers is given by second moment tensor,

$$\mathbf{A} = \oint \psi(\mathbf{p})\mathbf{p}\mathbf{p}d\mathbf{p} \quad (5)$$

where $\psi(\mathbf{p})$ is the probability density distribution function over orientation space.

Tensor $\mathbf{A}_4$ is a fourth order orientation tensor, defined as:

$$\mathbf{A}_4 = \oint \psi(\mathbf{p})\mathbf{p}\mathbf{p}\mathbf{p}\mathbf{p}d\mathbf{p} \quad (6)$$

where this tensor is also symmetric. The acceptable calculation is obtained through the eigenvalue-based optimal fitting approximation of the orthotropic closure family. To handle this complicated tensor system, Tseng *et al.* developed the a new fiber orientation model to couple with Jeffery's hydrodynamic (HD) model, namely, the iARD-RPR model (known as Improved Anisotropic Rotary Diffusion model combined with Retarding Principal Rate model),

$$\dot{\mathbf{A}} = \dot{\mathbf{A}}_{\mathrm{HD}} + \dot{\mathbf{A}}_{\mathrm{iARD}}(C_I, C_M) + \dot{\mathbf{A}}_{\mathrm{RPR}}(\alpha) \quad (7)$$

where $\dot{\mathbf{A}}$ represents the material derivative of **A**. Parameters C_I and C_M describe the fiber-fiber interaction and fiber-matrix interaction, while parameter α can slow down a response of fiber orientation. *Details of the RPR model and the iARD model are available elsewhere* [1].

$$\dot{\mathbf{A}}_{\mathrm{HD}} = (\mathbf{W}\cdot\mathbf{A} - \mathbf{A}\cdot\mathbf{W}) + \xi(\mathbf{D}\cdot\mathbf{A} + \mathbf{A}\cdot\mathbf{D} - 2\mathbf{A}_4 : \mathbf{D}) \quad (8)$$

where **W** and **D** are vorticity tensor and rate-of-deformation tensor, respectively. ξ is a shape factor of a particle. Such a model has been applied in CAE software of injection molding, **Moldex3D** (copyrighted by CoreTech System, Inc)

III. Fiber breakage model

A mean fiber length is described by number average L_N and weight average L_W, as follows:

$$L_N = \frac{\sum_{i=1}^{N} N_i l_i}{\sum_{i=1}^{N} N_i} \quad (8)$$

$$L_W = \frac{\sum_{i=1}^{N} N_i l_i^2}{\sum_{i=1}^{N} N_i l_i} \quad (9)$$

where N_i represent the expected value of the number of fibers of length l_i in a sample taken from a small region. Note that $l_i = i\Delta l$, Δl is the discretized length segment, namely, $\Delta l = L/N$, L is the initial length, N is number of segment. Regarding the related parameters, please refer to Ref. [2-3, 5]

IV. Fiber migration model

The suspension balance model [6-7] is considered for the suspension flow of rigid spherical particles in a Newtonian fluid. The particle phase is approximated as a pseudo-continuum. The dominant interaction between the particles includes hydrodynamics, viscous, non-Brownian forces with no external field except gravity.

Averaging over the particulate volume, the particle-phase conservation equation is given, as below,

$$\frac{\partial\phi}{\partial t} + \langle\mathbf{u}\rangle\cdot\nabla\phi = -\nabla\cdot\mathbf{j}_\perp \quad (10)$$

$$\mathbf{j}_\perp = \phi(U - \langle\mathbf{u}\rangle) \quad (11)$$

where ϕ is the particle volume fraction, $\langle\mathbf{u}\rangle$ is the suspension average velocity $\mathbf{j}_\perp$ is the particle flux relative to the mean suspension motion, and U is the local average velocity of the particulate phase. The detailed description of this model, please refer to our previous paper [6].

Furthermore, in suspension rheology, the viscosity η is function of shear rate of shear rate $\dot{\gamma}$, temperature T, pressure P, and particle concentration ϕ, namely,

$$\eta'(T,P,\dot{\gamma}) = \frac{\eta_o(T,P)}{1+\left(\eta_o\dot{\gamma}/\tau^*\right)^{1-n}} \quad (12)$$

$$\eta_o(T,P) = D_1\exp\left(\frac{-A_1(T-T_c)}{A_2+(T-T_c)}\right) \quad (13)$$

$$T_c = D_2 + D_3 P \quad (14)$$

$$A_2 = \tilde{A}_2 + D_3 P \quad (15)$$

where n is the power law index; τ^* is describes the transition region between the zero-shear-rate plateau and the power law region; D1, D2, D3, A1, and $\tilde{A}_2$, are the experimental fitting parameters.

Moreover, we can obtain,

$$\eta = \eta'(\dot{\gamma}, T, P)\eta_r(\phi) \quad (16)$$

where $\eta_r(\phi)$ is relative viscosity in dimensionless dependence of particle concentration of volume fraction. Also, it is the ratio of the suspension viscosity to the suspending liquid viscosity. $\eta_r(\phi)$ is simply defined,

$$\eta_r(\phi) = \left(1 - \frac{\phi}{\phi_m}\right)^{-2} \quad (17)$$

Investigation Model and Information

The geometry design is shown as in **Figure 1**. It is constructed based on ASTM D638 with dimension of 165mm×19mm×3mm. The moldbase and cooling channel layout is listed in **Figure 2**. The injection molding process setting is listed in Table 1 with filling 0.1 sec, packing 5.65 sec, cooling 15 sec, and other parameters. Material is Polykemi Polyfill PP (25% glass fiber). To catch the microstructure variations of fibers through the runner and cavity, the measuring nodes are specified as shown in **Figure 3**. Here it is specified as three regions for observation: near the gate (x=22.5 mm), center region (x=82.5 mm), and the end of filling region (x=142.5 mm), respectively. For each region, we have assigned three measuring nodes for observation. In addition, to examine the change of fiber length, three kinds of fiber length (1.7mm, 11.9mm, and 17.0mm) are considered. To cover full injection molding process with fiber microstructures variation, including fiber length, fiber orientation, and fiber density distribution, Moldex3D software are used to simulate.

Results and Discussion

Figure 4 shows the fiber orientation along the thickness direction near the gate region. The key parameters are orientation tensor components: $\mathbf{a_{11}}$, $\mathbf{a_{22}}$, and $\mathbf{a_{33}}$ corresponding to the flow, the cross-flow, and thickness directions, respectively. As shown in **Figure 4(b)**, a high value of $\mathbf{a_{11}}$ will indicate a large fraction of fibers oriented in the flow direction, while a near-zero value of $\mathbf{a_{33}}$ will indicate little or no orientation in the thickness direction. In addition, the transition point will be the interface between the skin layer and core layer. Besides, from **Figure 4(a) and (c)**, the core layer shows the high value of $\mathbf{a_{11}}$ indicates a large fraction of fibers oriented in the flow direction. Clearly, **Figure 4(a)** and **(c)** show significant difference with that of **(b)**. Moreover, in **Figure 5(a)**, when it flows from location B to H, $\mathbf{a_{11}}$ is originally in high and board to low and narrow values, and then becomes high and board value again. At the same time, in **Figure 5(a)**, $\mathbf{a_{22}}$ shows the opposite behavior than that of $\mathbf{a_{11}}$. Obviously, **Figure 5** shows that the geometrical structure can provide significant effect on the fiber orientation.

Furthermore, to investigate the change of fiber length during the injection process, original fiber lengths 1.7 mm (short fiber, SF), 11.9 mm (medium fiber, MF), and 17 mm (long fiber, LF) are applied to enter the sprue entrance as shown in **Figure 1**. **Figure 6** shows the fiber length distribution along the thickness direction near the gate region. In **Figure 6(b)**, for LF, the fiber length (close to the top or bottom skin) is reduced to 1.15 mm, while it is 12.36 mm in the center of core layer. In **Figure 6(a)** or **(c)**, for LF, the fiber length close to the top or bottom skin is reduced to 1.145 mm, while it is 6.535 mm in the center of core layer. Obviously, no matter how long the original fiber, the fiber length on the skin layer is almost reduced to equal or smaller than 1 mm. And when we focused on the core layer through the flow along the **a** or **c** location the long fibers have been damaged significantly. Moreover, **Figure 7(a)** shows the fiber length distribution of the skin layer along the flow direction in the cavity. Due to the geometrical contraction and expansion, the flow field reformed and the fiber length distribution is from 0.4 mm to 3.1 mm for the long fiber through the skin layer. Specifically, there is very sharp fiber length reduction (almost 90% length is broken) happened around the gate. It is due to the high shear force generated when melt is converged into the very small gate entrance. Meanwhile, **Figure 7(b)** exhibits the fiber lengths along the core layer. Although the change looks smoothly, the average fiber lengths are 12 mm for LF, 8 mm for MF, and 1.25 mm for SF respectively. Indeed, 30% of original fiber lengths are missed. To search for the reason why some fiber lengths are missed, the journey of the fiber is extended to the runner section. **Figure 8** shows the fiber length distribution from the sprue, to runner, and to cavity. Clearly, there is a dramatically change of fiber length during the melt went through the runner section. In this benchmark, the breakage percentage during the journey of runner is about 30% for LF and MF.

Moreover, to valid our numerical simulation results, we have adopted some results from Ref. [4] although resin they applied is PBT. **Figure 9** shows the locations for observation on the fiber orientation for both cases. **Figure 10** displays the comparison on the fiber orientation tensors between this work and Ref. [4] at near the gate region. From the skin layer to core layer, all orientation tensors are in a pretty good agreement in trend. When further consider the fiber orientation down-stream as shown in **Figure 11**, the trend is still in good agreement.

Conclusions

In this study, we have performed a benchmark to consider three different lengths of fiber thermoplastic composites based on ASTM D638 with dog-bond structure. Results showed that the geometry of cavity has significant effect on the fiber orientation during the injection processes. When the geometry of the system has contraction and expansion structure, the orientation tensor component $\mathbf{a_{11}}$ corresponding to the flow direction, will be enhanced and then decreased. Moreover, the fiber lengths have dramatically sharp distribution on skin layer when melt goes through the gate into the cavity. It will allow almost 90% lengths are broken through the skin layer. Meanwhile, using numerical visualization from runner to cavity through core layer, there is about 30% length broken during the journey in runner section. Finally, some fiber orientation results are compared with literature's. Results showed that our numerical predictions are matched with that of literature quite well in the trend.

Acknowledgements

The authors would like to thank Ministry of Science and Technology of Taiwan, R.O.C. (Project number: MOST 105-2622-E-006-0035-CC1) for financially supporting for this research.

References

1. Advani, S.G., 1994. *Flow and Rheology in Polymer Composites Manufacturing* (Elsevier, New York)
2. Tseng, H.-C., R.-Y. Chang, and C.-H. Hsu, "Phenomenological improvements to predictive models of fiber orientation in concentrated suspensions." *J. Rheol.* 57 1597 (2013).
3. Tseng, H.-C., R.-Y. Chang, and C.-H. Hsu, "Method and computer readable media for determining orientation of fibers in a fluid," *U.S. Patent* No. 8571828 (2013).
4. Peter H. Foss, Huan-Chang Tseng, John Snawerdt, Yuan-Jung Chang, Wen-Hsien Yang, Chia-Hsiang Hsu, "Prediction of Fiber Orientation Distribution in Injection Molded Parts Using Moldex3D Simulation", *Polym. Compos.*, 35, 4, pp. 671-680 (2014).
5. Phelps, J.H., Abd El-Rahman, A.I., Kunc, V., and Charles L. Tucker, I., *Composites Part A: Applied Science and Manufacturing* **51** 11-21 (2013)
6. Tseng, H.-C., C.-H. Hsu, and R.-Y. Chang, SPE ACCE (2014)
7. Morris, J. F. and F. Boulay, "Curvilinear flows of noncolloidal suspensions: The role of normal stresses." *J. Rheol.* 43 1213-1237 (1999).
8. Seropе Kalpakjian and Steven R. Schmid , Chaper 9, Manufacturing, Engineering & Technology, Fifth Edition.
9. Chao-Tsai (CT) Huang; Huan-Chang Tseng; Rong-Yeu Chang; Sheng-Jye Hwang, *SPE Technical Papers, ANTEC2016*, pp.1120-1125 (2016).
10. Alexander Roch, A. Menrath, T. Huber, F. Henning, and P. Elsner, *Cellular Polymers*, 32, No. 4, pp. 214-228 (2013)
11. Jeff Webb and Li Qi, SPE Technical Papers, *SPE Technical Papers,* ANTEC2013, Paper No. 1591663 (2013).

Table 1. Process condition setting

Item	Condition Setting
Material	Polykemi AB PP (25% GF)
Filling time	0.1 s
Packing time	5.65 s
Cooling time	15 s
Open and close	5 s
Melting temperature	220 °C
Mold temperature	40 °C
Air temperature	25 °C
Packing pressure	70% of the injection pressure at the end of filling

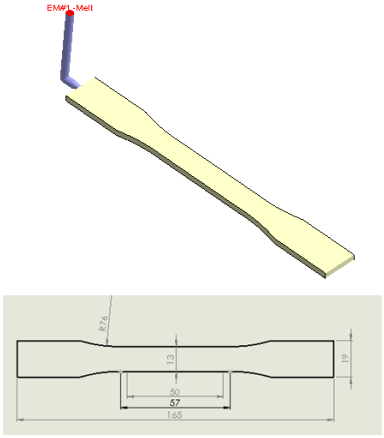

Figure 1. The part geometry based on ASTM D638.

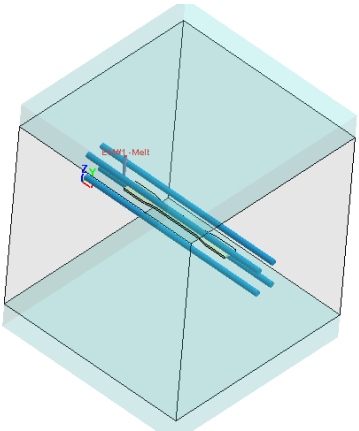

Figure 2. the moldbase and cooling channel layout.

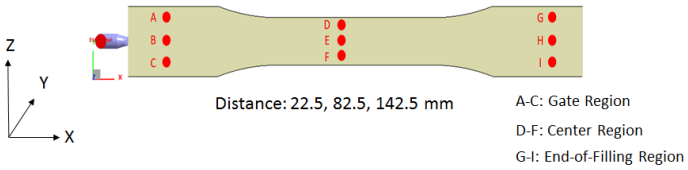

Figure 3. The observation locations.

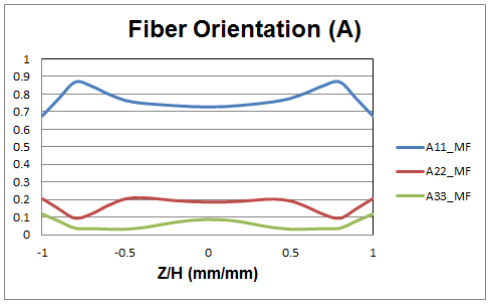

(a)

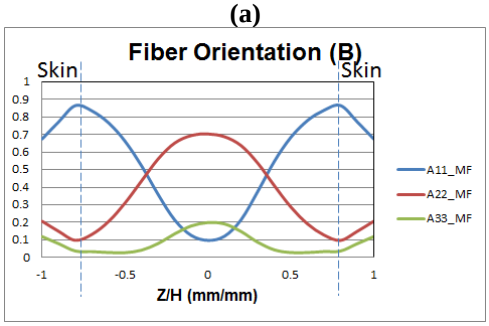

(b)

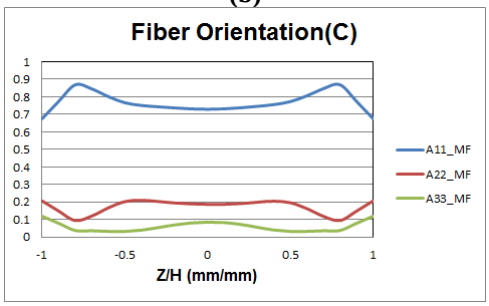

(c)

Figure 4. Fiber orientation along thickness direction near the gate region, where MF: medium fiber = 11.9 mm.

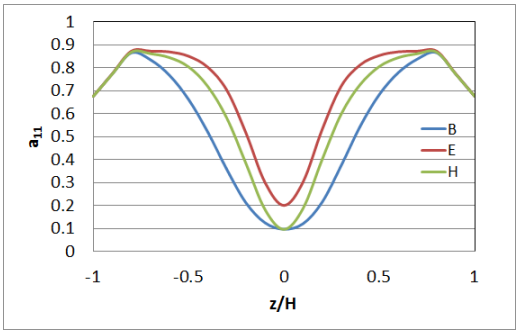

(a)

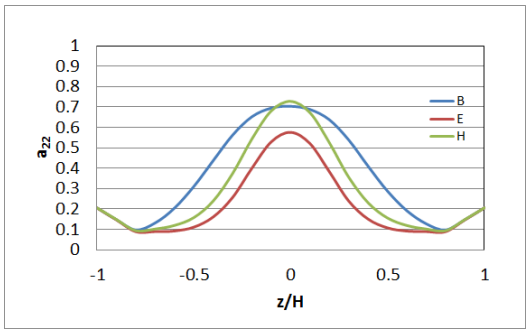

(b)

Figure 5. Fiber orientation from up to down-stream in the flow direction: (a) a11, (b) a22.

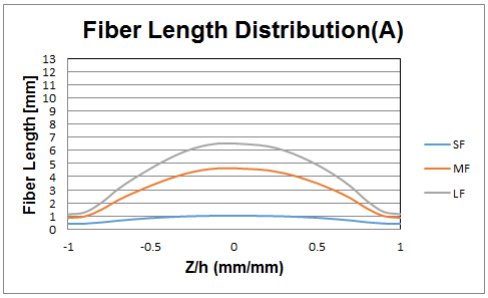

(a)

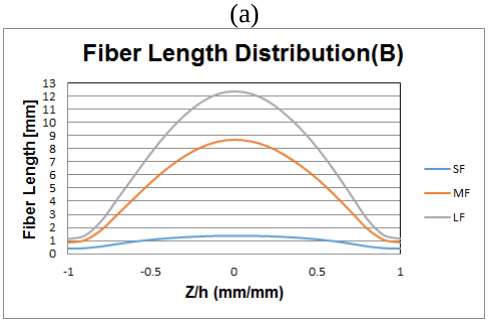

(b)

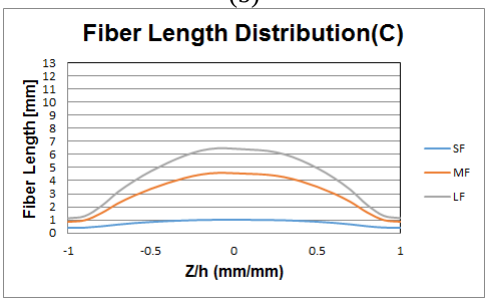

(c)

Figure 6. Fiber length distribution along the thickness direction near the gate region, where SF is short fiber, MF is medium fiber, LF is long fiber.

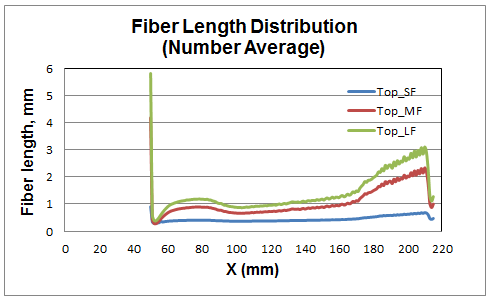

(a)

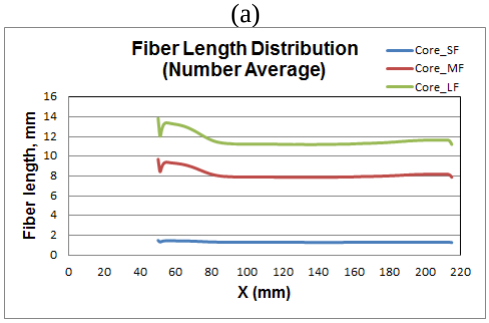

(b)

Figure 7. Fiber length distribution along the flow direction in cavity: (a) on skin layer, (b) in the core layer.

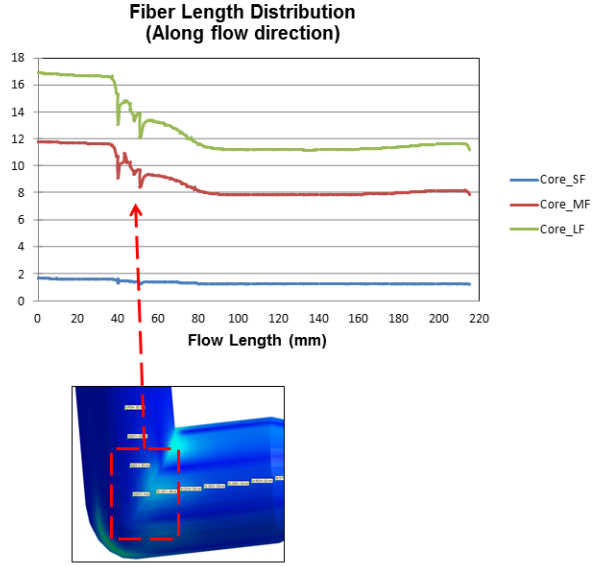

Figure 8. Fiber length variation through the runner section.

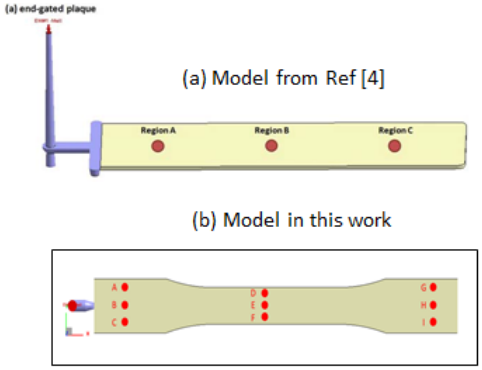

Figure 9. Models for validation purpose.

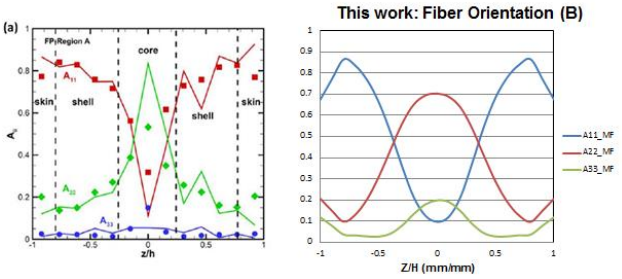

(a) Ref [4]: Region A, (b) This work: location B

Figure 10. The comparison of the fiber orientation.

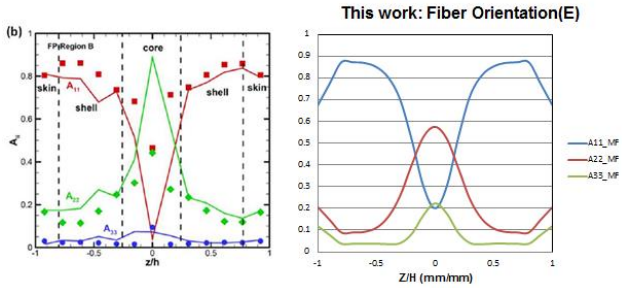

(a) Ref [4]: Region B, (b) This work: location E

Figure 11. The comparison of the fiber orientation.